Dependence of interatomic decay widths on the symmetry of the decaying state: Analytical expressions and *ab initio* results

K. Gokhberg,[1] S. Kopelke,[1] N. V. Kryzhevoi,[1] P. Kolorenč,[2] and L. S. Cederbaum[1]

[1]*Theoretische Chemie, Physikalisch-Chemisches Institut, Universität Heidelberg, Im Neuenheimer Feld 229, D-69120 Heidelberg, Germany*
[2]*Institute of Theoretical Physics, Faculty of Mathematics and Physics, Charles University in Prague,*
V Holešovičkách 2, CZ-18000, Prague, Czech Republic

In this article, we investigate the dependence of interatomic Coulombic decay widths on the symmetry of the decaying state. In this type of decay, excited, ionized, and doubly ionized states of an atom or molecule can efficiently relax by ionizing their environment. We concentrate on an atom A and a neighboring atom B and consider such excited, ionized, or doubly ionized states of A that decay by emitting a single photon if A were an isolated atom. Analytical expressions for the various widths are derived for large interatomic distances R. A pronounced dependence of the widths on the symmetry properties of the decaying state is found. This dependence at large R is related to the dependence of the interaction energy of two classical dipoles on their mutual orientation. Comparison with precise *ab initio* calculations shows that the analytical results hold well at large R, while they deviate from the *ab initio* values at smaller R due to the effect of orbital overlap.

I. INTRODUCTION

Interatomic Coulombic decay (ICD) is an extremely efficient relaxation process taking place in weakly bound systems, whereby an electronic excitation localized on one unit decays on a femtosecond time scale by ionizing neighboring atoms or molecules. Originally ICD was predicted [1] and investigated both theoretically and experimentally [2–7] in singly ionized clusters, where one of the constituent monomers had a hole in an inner-valence shell. Later investigations showed that it exists also in excited neutral clusters [8–11] and in excited doubly ionized clusters that are produced via an Auger decay on one of the monomers [12–17]. Thus, there seems to be no restrictions on the nature of the initially excited state and interatomic decay takes place as long as the corresponding channel is energetically accessible.

Among several characteristics of interatomic decay, its decay width Γ is of central importance. Since ICD, in principle, can be accompanied by other decay processes, photon emission or autoionization to name a few, knowledge of Γ allows one to decide how important interatomic decay is for a given excited state in the cluster of interest. Extensive *ab initio* calculations of interatomic decay widths have been performed for a number of systems, e.g., Ne_n [2], MgNe [9], and NeAr [17]. These calculations not only produced values of Γ for the equilibrium nuclear configurations of clusters under study but also demonstrated the behavior of Γ as a function of interatomic distances in clusters and the number of monomers surrounding the excited moiety. However, for some excited states the decay width might depend on an additional parameter, as we illustrate below on the example of ICD in the CaHe cluster.

Let us assume that the initial excitation is produced by removing an electron from the $3p$ shell of Ca atom. The resulting $Ca^+(3p^{-1})He$ cluster might decay by the ICD mechanism, whereby an electron from the $4s$ shell of Ca fills the initial vacancy, while in a concerted step an electron is removed from the $1s$ shell of the He atom into the continuum. The initial state of the system is derived from the $^2P^o$

term of the Ca atom and the ^1S ground state of the He atom. The $^2P^o$ term has three components corresponding to different projections of the orbital angular momentum which are energetically degenerate in an isolated atom. In the Ca^+He cluster the degeneracy of this term is partially lifted, giving rise to a nondegenerate $^2\Sigma^+$ and a doubly degenerate $^2\Pi$ state. By choosing light polarized either along or perpendicular to the interatomic axis, one can selectively prepare a state of either $^2\Sigma^+$ or $^2\Pi$ symmetry which is the initial state of the ICD process. *Ab initio* calculations produced the surprising result [18] that the decay width of the state of $^2\Sigma^+$ symmetry can be as much as four times larger than the decay width of the state of $^2\Pi$ symmetry. Moreover, this ratio persists even if the two atoms are infinitely far apart and the states $^2\Sigma^+$ and $^2\Pi$ become degenerate. A dependence of Γ on the symmetry of the initially excited state was also found in the results of *ab initio* calculations with neutral or doubly ionized initial states. Since this phenomenon has never been satisfactorily explained in the framework of ICD, we attempt to do it in the present article.

We investigate the effect of the initial state's symmetry in weakly bound heteronuclear clusters AB on the interatomic decay width for different types of initial excitations which include excited cations and dications as well as excited states of the neutrals. We analyze the nature of this dependence by deriving analytical expressions for the decay widths at large interatomic separations R. In those cases where the initial state can decay in the isolated atom by single-photon emission according to dipole selection rules the decay at large interatomic distances proceeds through energy (virtual photon) transfer. The corresponding decay widths exhibit a $1/R^6$ behavior with a prefactor which is a product of quantities pertaining to the isolated atoms A and B. We show that the width's dependence on the symmetry of the initial state appears in the prefactor and can be traced back to a classical phenomenon: the dependence of the interaction energy of two dipoles on their mutual orientation. The validity of asymptotic expressions, first derived in the context of interatomic Auger decay in

Ref. [19], was investigated by Averbukh *et al.* [4] who showed that at distances considerably larger than the equilibrium distance the $1/R^6$ dependence holds well, while at distances about equilibrium it can break down due to the effect of orbital overlap. Averbukh *et al.* [4] did not investigate the dependence of ICD decay widths on the symmetry of the initial state, since the considered initial states which can decay by dipole transitions in the isolated atom were of Σ symmetry. In addition to these, they also studied cases where the initial state's decay in the isolated atom is dipole forbidden and discussed the respective $1/R^8$ and $1/R^{10}$ asymptotic behavior of the ICD widths. In the present work we generalize and complement their study by showing that the prefactor multiplying the $1/R^6$ term depends on the initial state's symmetry. We then compare asymptotic decay widths to Γ's computed using precise *ab initio* methods in order to see whether the dependence on symmetry at large R is indeed as predicted by asymptotic formulas and to determine the effect of orbital overlap on this dependence in the vicinity of the equilibrium distance.

The plan of this article is as follows. In the next section we sketch the derivation of the asymptotic expressions of the interatomic Coulombic decay widths for various types of initial states, while a more detailed derivation can be found in the Appendix. Comparison with *ab initio* calculations in several systems will be given in Sec. III together with a discussion of the results obtained. Conclusions are presented in Sec. IV. We use atomic units everywhere in this article unless indicated otherwise.

II. DERIVATION OF ASYMPTOTIC FORMULAE

We start by deriving asymptotic formulas for the interatomic decay of an inner-valence vacancy on atom A of the cluster AB. The derivations in the case of doubly ionized and neutral clusters are similar and will be outlined next. We assume first that the one-particle spin orbitals were obtained previously, e.g., by solving Hartree-Fock equations. In a heteroatomic system bound orbitals tend to be localized on either A or B as the interatomic distance grows and they asymptotically approach the bound orbitals of the isolated atoms A and B. This reasoning apparently fails in the case of continuum orbitals which remain delocalized no matter how large the interatomic distance. However, as we will see later, it is not these orbitals by themselves which are important but matrix elements of some operators evaluated between continuum orbitals and orbitals localized on a given atom. The part of the continuum orbital contributing most to such matrix elements is indistinguishable asymptotically from the corresponding part of the continuum orbital obtained for the isolated atom. Therefore, we designate all orbitals by $|\gamma l m \mu\rangle$, where l, m, μ, and γ stand for the orbital angular momentum, its projection on the intermolecular axis, projection of the electron spin, and the rest of quantum numbers, respectively. In what follows we assume the intermolecular axis to be aligned along the z axis. The bound and continuum orbitals satisfy the following normalization conditions

$$
\begin{aligned}
\langle \gamma' l' m' \mu' | \gamma l m \mu \rangle &= \delta_{\gamma \gamma'} \delta_{ll'} \delta_{mm'} \delta_{\mu \mu'} \\
\langle \gamma' l' m' \mu' | \gamma l m \mu \rangle &= \delta(\epsilon_{\gamma' l'} - \epsilon_{\gamma l}) \delta_{ll'} \delta_{mm'} \delta_{\mu \mu'}
\end{aligned}
\tag{1}
$$

where $\epsilon_{\gamma l}$ stands for the energy of a continuum state. We next assume for simplicity of presentation that the single determinant ground state $|\Phi_0\rangle$ of the system was constructed and that it is closed shell, i.e., a $^1\Sigma$ term. In addition, we assume that the ground states of the atoms A and B are also closed shell and consequently are ^1S terms. We make this assumption since the majority of systems of current experimental interest, e.g., noble gas or rare earth-noble gas clusters, belong to this class. The generalization of the following results to systems with ground states of different symmetry is straightforward. Moreover, as long as the system is closed shell in its ground state, one can easily extend the theory to the fully correlated ground state $|\Psi_0\rangle$.

A. Singly ionized atom A

In the case of the singly ionized atom A the initial vacancy resides in the inner-valence shell iv. After ICD one obtains doubly ionized cluster AB with one hole in the outer-valence shell ov_A localized on the atom A, another in the outer-valence shell ov_B located on the atom B, and an electron ejected from the atom B into the continuum. A schematic representation of this process is given in Fig. 1(a).
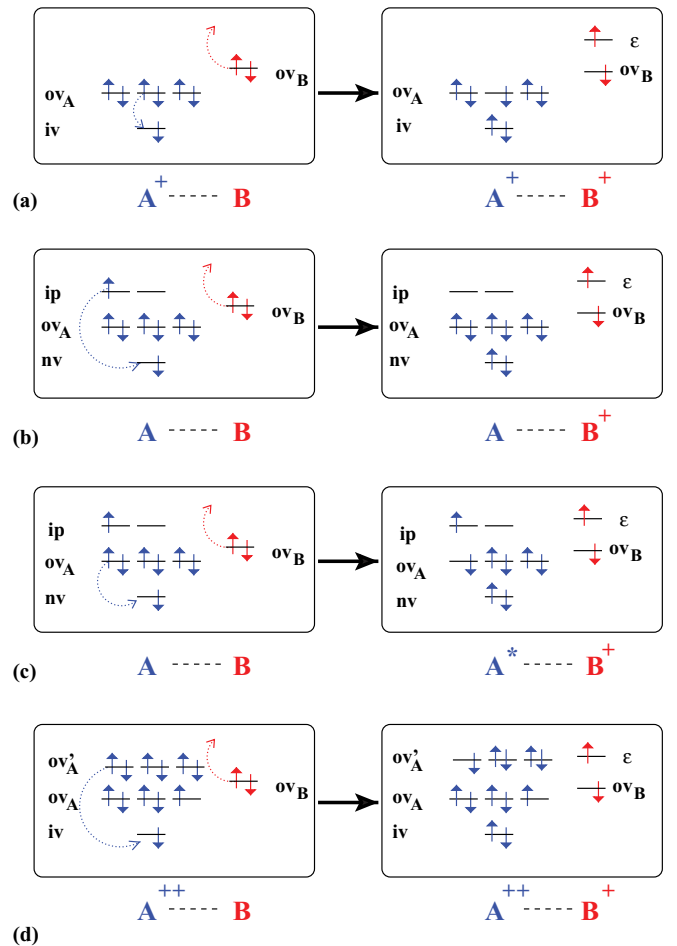

FIG. 1. (Color online) Schematic descriptions of the interatomic decay processes discussed in the text for a dimer A···B with an initially excited or ionized atom A. (a) ICD, (b) pRICD/ETI, (c) sRICD, (d) ICD after Auger decay. The symbol "ov" stands for outer valence, "iv," inner valence; "nv," either outer or inner valence; and "ip" for a particle (virtual) orbital.

The initial state of the system is obtained by removing an electron from the inner-valence orbital $|\alpha_{\rm iv} l_{\rm iv} m_{\rm iv} \mu_{\rm iv}\rangle$ localized on atom A. The corresponding single determinant many-electron function is given by

$$|E L_A M_A S M_S\rangle = \hat{c}_{\alpha_{\rm iv}}|\Phi_0\rangle, \qquad (2)$$

where $\hat{c}_{\alpha_{\rm iv}}$ is the annihilation operator for the electron in the respective inner-valence orbital. In specifying the initial state of AB, $|E_{\rm in} L_A M_A S M_S\rangle$, we use the following quantum numbers: the energy of the initial state E, and the orbital angular momentum $L_A = l_{\rm iv}$ and its projection on the z axis $M_A = -m_{\rm iv}$ which the atom A would have were it isolated. Since the system possesses only axial symmetry, only $M_{\rm iv}$ is an exact quantum number. We assume, however, that at large interatomic separations $L_{\rm iv}$ remains a good quantum number too. By removing one electron from a closed-shell ground state of AB we obtain the total spin $S = 1/2$, while M_S stands for its projection on the z axis.

The final state of the interatomic Coulombic decay of an inner-valence vacancy is obtained by removing electrons from the outer-valence orbitals $|\alpha_{{\rm ov}_A} l_{{\rm ov}_A} m_{{\rm ov}_A} \mu_{{\rm ov}_A}\rangle$ and $|\beta_{{\rm ov}_B} l_{{\rm ov}_B} m_{{\rm ov}_B} \mu_{{\rm ov}_B}\rangle$ localized on A and B, respectively, and creating an electron in the continuum orbital $|\beta_\epsilon l_\epsilon m_\epsilon \mu_\epsilon\rangle$. The resulting one-determinant state is expressed mathematically by

$$\left|\beta_\epsilon \alpha_{{\rm ov}_A} \beta_{{\rm ov}_B}\right\rangle = \hat{c}^\dagger_{\beta_\epsilon} \hat{c}_{\alpha_{{\rm ov}_A}} \hat{c}_{\beta_{{\rm ov}_B}} |\Phi_0\rangle. \qquad (3)$$

Next, we bring the final state given in Eq. (3) into the same form as the initial state given in Eq. (2). First, unlike the initial state it is not an eigenstate of the total spin operator. A spin doublet state can be constructed from an one-particle–two-hole (1p2h) state in Eq. (3) in two different ways. One can add the spins of the two holes to form a singlet and then add the spin of the particle in continuum to form a doublet. Alternatively one adds the spins of the holes to form a triplet to which adding the spin of the particle gives $S = 1/2$. The spin states constructed in this way allow for a simple interpretation: once the ejected electron is removed from the system the remaining doubly ionized cluster is either in the spin singlet or spin triplet state. The spin eigenfunctions are given by

$$\left|\beta_\epsilon \alpha_{{\rm ov}_A} \beta_{{\rm ov}_B}; S'_N M'_S\right\rangle = \sum_{\mu_\epsilon \mu_{{\rm ov}_A} \mu_{{\rm ov}_B}} C^{S'_N M'_S}_{\mu_\epsilon \mu_{{\rm ov}_A} \mu_{{\rm ov}_B}} \left|\beta_\epsilon \alpha_{{\rm ov}_A} \beta_{{\rm ov}_B}\right\rangle, \qquad (4)$$

where $C^{S'_N M'_S}_{\mu_\epsilon \mu_{{\rm ov}_A} \mu_{{\rm ov}_B}}$ are spin coupling coefficients and the superscript N enumerates the different ways to construct spin doublet states. One obtains the spin coupling coefficients either as a product of Clebsch-Gordan coefficients, if using the standard angular-momentum addition formulas in constructing the spin eigenstates [20], or in some other form, if using specialized construction schemes [21].

Second, we apply an additional unitary transformation to the states in Eq. (4) to obtain $|E' L'_A M'_A L'_B M'_B S'_N M'_S\rangle$, where, analogously to the case of the initial state, E' is the energy of the final state, and L'_A, M'_A, and L'_B, M'_B are the orbital angular momenta and their projections on the z axis which the atoms A and B would have, if isolated. Again, M_A, M_B are exactly conserved quantities, while L'_A, L'_B will be good quantum numbers asymptotically. We see that in our case $L'_A = l_{{\rm ov}_A}$ and $M'_A = -m_{{\rm ov}_A}$. To obtain L'_B and M'_B we have to add

the momenta l_ϵ and $l_{{\rm ov}_B}$. According to the rules of angular-momentum addition allowed values of L_B are those satisfying $|l_\epsilon - l_{{\rm ov}_B}| \leqslant L'_B \leqslant l_\epsilon + l_{{\rm ov}_B}$ and $M'_B = m_\epsilon - m_{{\rm ov}_B}$. Thus we obtain for the states of interest

$$|E' L'_A M'_A L'_B M'_B S'_N M'_S\rangle = \sum_{m_\epsilon m_{{\rm ov}_B}} C^{L'_B M'_B}_{m_\epsilon m_{{\rm ov}_B}} \left|\beta_\epsilon \alpha_{{\rm ov}_A} \beta_{{\rm ov}_B}; S'_N M'_S\right\rangle, \qquad (5)$$

where $C^{L'_B M'_B}_{m_\epsilon m_{{\rm ov}_B}}$ are vector coupling coefficients expressed through the standard Clebsch-Gordan coefficients of the rotation group [20] [see Eq. (A4)].

The initial and final states are coupled by electron-electron interaction

$$\hat{V}_e = \frac{1}{2} \sum_{i \neq j} \frac{1}{|\mathbf{r_i} - \mathbf{r_j}|}, \qquad (6)$$

where $\mathbf{r}_i$ denotes the coordinates of the ith electron. The decay width is given by the golden rule, see, e.g., Ref. [22],

$$\Gamma = 2\pi \sum |\langle E' L'_A M'_A L'_B M'_B S'_N|\hat{V}_e|E L_A M_A S\rangle|^2 \delta(E' - E), \qquad (7)$$

where the sum runs over all final states and the delta function ensures conservation of energy in the decay process. We also average over different spin projections in the initial state and omit them in the expressions to follow.

At large interatomic distances a state of AB can be represented as the product of states of the isolated A and B. Thus, the ground state $|\Phi_0\rangle \rightarrow |\Phi_0^{(A)}\rangle |\Phi_0^{(B)}\rangle$, $|E L_A M_A S\rangle \rightarrow |E_A L_A M_A S\rangle |\Phi_0^{(B)}\rangle$, and $|E' L'_A M'_A L'_B M'_B S'_N\rangle \rightarrow |E'_A L'_A M'_A S'_A\rangle |E'_B L'_B M'_B S'_B\rangle$, where $E = E_A + E_B$ and $E' = E'_A + E'_B$. The states of the isolated atoms A and B are constructed completely analogously to the states in Eq. (5), with the only difference that in doing so one should use the single determinant ground states of isolated atoms A and B, $|\Phi_0^{(A)}\rangle$ and $|\Phi_0^{(B)}\rangle$, instead of $|\Phi_0\rangle$. These atomic ground states can, in their turn, be constructed from spin-orbitals $|\gamma l m \mu\rangle$ localized either on the atom A or on the atom B. As we show in detail in the Appendix, under these conditions the decay amplitude in Eq. (7) can be represented as the sum of products of amplitudes of the processes occurring on separated atoms which are the deexcitation of atom A and the ionization of atom B

$$\langle E' L'_A M'_A L'_B M'_B S'_N|\hat{V}_e|E L_A M_A S\rangle$$
$$= \frac{C_N}{\sqrt{2}} \sum_{l=0}^\infty \sum_{m=-l}^l \left\langle E'_A L'_A M'_A S'_A\right|\hat{D}^{(A)}_{lm}\left|E_A L_A M_A S\right\rangle$$
$$\times \left\langle \Phi_0^{(B)}\right|\hat{D}^{(B)}_{lm}\left|E'_B L'_B M'_B S'_B\right\rangle^*, \qquad (8)$$

where $C_1 = 1/\sqrt{2}$ and $C_2 = \sqrt{3/2}$ and the operators $\hat{D}_{lm}$ are given by

$$\hat{D}^{(A)}_{lm} = \sqrt{\frac{4\pi}{2l+1}} \sum_{i \in A} Y_{lm}(\Omega_i) r_i^l \qquad (9a)$$

$$\hat{D}^{(B)}_{lm} = \sqrt{\frac{4\pi}{2l+1}} \sum_{j \in B} Y_{lm}(\Omega_j)/r_j^{l+1} \qquad (9b)$$

where the sums run over all electrons localized either on A or on B, respectively. The spin of A is $S'_A = 1/2$ and the spin of B is $S'_B = 0$.

If the transition between the states $|E_A L_A M_A S\rangle$ and $|E'_A L'_A M'_A S'_A\rangle$ of the atom A is dipole allowed then the leading term in Eq. (8) is the one with $l = 1$

$$\langle E' L'_A M'_A L'_B M'_B S'_N | \hat{V}_e | E L_A M_A S \rangle$$
$$= \frac{C_N}{\sqrt{2} R^3} \sum_{m=-1}^{1} B_m \langle E'_A L'_A M'_A S'_A | \hat{D}_m^{(A)} | E_A L_A M_A S \rangle$$
$$\times \left\langle \Phi_0^{(B)} | \hat{D}_m^{(B)} | E'_B L'_B M'_B S'_B \right\rangle^*, \qquad (10)$$

where we introduce the notations for the dipole operators $\hat{D}_m^{(A,B)} = \sum_{i \in (A,B)} r_m^{(i)}$. The dipole-dipole product terms in the sum in Eq. (10) are multiplied by constants $B_0 = -2$ and $B_{\pm 1} = 1$. We see that the transition driven by the projection of the dipole operator parallel to the intermolecular axis contributes to the decay amplitude twice as much as the one driven by the projection of $\hat{D}$ perpendicular to z axis. Precisely this phenomenon leads to different decay widths of the cluster states polarized along or perpendicular to the z axis.

This phenomenon is surprising at first sight because it holds even at very large interatomic separations. We are going to show below that it has a classical explanation. Indeed, the interaction energy between two classical dipoles with dipole moments $\mathbf{p}_1$ and $\mathbf{p}_2$ located at coordinates $\mathbf{x}_1$ and $\mathbf{x}_2$ is given by [23]

$$W = \frac{\mathbf{p}_1 \cdot \mathbf{p}_2 - 3(\mathbf{n} \cdot \mathbf{p}_1)(\mathbf{n} \cdot \mathbf{p}_2)}{|\mathbf{x}_1 - \mathbf{x}_2|^3}, \qquad (11)$$

where $\mathbf{n}$ is an unit vector parallel to $\mathbf{x}_1 - \mathbf{x}_2$, i.e., parallel to the line connecting the two dipoles. As we see from Eq. (11), if both $\mathbf{p}_1$ and $\mathbf{p}_2$ are aligned parallel to $\mathbf{n}$ the interaction energy is twice the interaction energy of the dipoles parallel to each other but perpendicular to $\mathbf{n}$. Moreover, this ratio remains the same for all separations between the dipoles. We see that apart from a constant factor Eq. (10) can be obtained from Eq. (11) by replacing classical dipole moments through the transition dipole amplitudes of the two atoms.

Substituting the term in Eq. (10) into Eq. (7) we obtain for Γ

$$\Gamma = \frac{2\pi}{R^6} \sum B_{M'_A - M_A}^2 \delta(E' - E)$$
$$\times \left| \langle E'_A L'_A M'_A | \hat{D}_{M'_A - M_A}^{(A)} | E_A L_A M_A \rangle \right.$$
$$\times \left\langle \Phi_0^{(B)} | \hat{D}_{M'_A - M_A}^{(B)} | E'_B L'_B M_A - M'_A \rangle \right|^2, \qquad (12)$$

where we suppressed the spin variables. To derive Eq. (12) we also used the following considerations. First, since we assumed that the ground state of B is ^1S the sum in Eq. (10) contains only a single nonvanishing term with $m = -M'_B$ and the only allowed value of L'_B is unity. Second, the system is axially symmetric and $M'_A + M'_B = M_A$. We would also like to note here that the energy conservation expressed by the delta function will be satisfied for all energies of the initial state, once ICD channel opens. This is due to the fact that the energy eigenvalues of the emitted ICD electron taking the excess energy in the decay is not quantized. The expression in Eq. (12) can be recast in terms of measurable parameters

of the isolated atoms. Asymptotically we can write $E' - E = \omega_A - \omega_B$, where $\omega_A = E_A - E'_A$ the energy released in the transition on the atom A, while $\omega_B = E'_B - E_B$ is the energy absorbed in the photoionization of the atom B. If the decay can proceed to different shells ov$_A$ or to the states in the same shell but having different angular momenta L'_A, then these channels will be characterized through the excitation energies $\omega_A^{(i)} = \omega_i$ and partial decay widths Γ_i. Since asymptotically ω_i is independent of M_A the expression for Γ_i can be given in a factorized form

$$\Gamma_i = \frac{2\pi}{R^6} \sum_{M'_A} B_{M'_A - M_A}^2 \left| \langle E'_A L'_A M'_A | \hat{D}_{M'_A - M_A}^{(A)} | E_A L_A M_A \rangle \right|^2$$
$$\times \frac{1}{3} \sum_{\omega_B} \left| (\Phi_0^{(B)} || \hat{D}^{(B)} || E'_B L'_B) \right|^2 \delta(\omega_i - \omega_B). \qquad (13)$$

The second sum in Eq. (13) extends over all states of B participating in the decay, and, therefore, this sum is just $3\sigma^{(B)}(\omega_i)c/4\pi^2\omega_i$ [24], where $\sigma^{(B)}(\omega_i)$ is the photoionization cross-section of the atom B at energy ω_i. In addition, using Wigner-Eckart theorem [20] in the first sum we obtain

$$\Gamma_i = \frac{c}{2\pi \omega_i R^6} P_{M_A} S_i^{(A)}(E'_A L'_A; E_A L_A) \sigma^{(B)}(\omega_i), \qquad (14)$$

where the quantity P_{M_A} is given by

$$P_{M_A} = \sum_{M'_A} B_{M'_A - M_A}^2 \left| \begin{pmatrix} L'_A & 1 & L_A \\ -M'_A & M'_A - M_A & M_A \end{pmatrix} \right|^2 \qquad (15)$$

and is clearly a function of M_A; that is, it depends on the symmetry of the initial state. The quantity $S(\gamma L; \gamma' L') = |(\gamma L || D || \gamma' L')|^2$ is called the line strength for the transition from the multiplet $|\gamma L\rangle$ to the multiplet $|\gamma' L'\rangle$. It is connected to the corresponding transition probability W through [25]

$$W = \frac{4\omega^3}{3c^3} \frac{1}{2L + 1} S(\gamma L; \gamma' L'). \qquad (16)$$

To obtain the total decay width one should sum over all partial widths

$$\Gamma = \sum_i \Gamma_i. \qquad (17)$$

The ICD process as given in Eq. (14) can be visualized using the concept of the "virtual" photon transfer [4]. Thus, the decay of the initial excitation on A and the photoionization of B are connected by the transfer of a "virtual" photon of energy ω_i whose polarization enters P_{M_A}. The effectiveness of this transfer falls off with the interatomic distance as $1/R^6$, due to the diminishing interaction between the atomic dipoles.

B. Doubly ionized atom *A*

The asymptotic decay widths for initial excited states of the neutral and doubly ionized atoms are given by expressions similar to those in Eq. (14). Therefore, we discuss here only the construction of the initial and final states and give the final expression for the decay width, while necessary details are found in the Appendix. We start with the case of doubly ionized states [12]. Such states can be produced in the Auger decay of a core vacancy in the atom A. Here, we consider the initial excitation to consist of two holes: one in an inner-valence shell iv

and another in an outer-valence shell ov_A [see Fig. 1(d)]. In the Auger decay both singlet and triplet spin states of the dication can be populated [26,27]. Moreover, as we demonstrate in the Appendix, both can decay by the energy transfer mechanism and, thus, have asymptotic widths falling off as $1/R^6$. To obtain the wave function of the initial excitation $|EL_A M_A S_A\rangle$ we add the spins and the orbital angular momenta of the holes in iv and ov_A shells separately for the triplet $S_A = 0$ and $S_A = 1$ states.

In the decay an electron from the orbital in the shell ov'_A, which may or may not coincide with ov_A, fills the vacancy in iv, while the atom B becomes ionized. Thus, in the final state there are three holes in orbitals in the shells ov_A, ov'_A, and ov_B and an electron in the continuum orbital ϵ [see Fig. 1(d)]. First, we add the spins of the three holes and the particle to obtain the total spin S'_N, where N numbers different spin genealogies, two for $S'_N = 0$ and three for $S_N = 1$. Second, we add the orbital angular momenta of the holes on A to obtain L'_A and M'_A, and of the particle and the hole on B to obtain L'_B and M'_B. We denote the resulting final state as $|E'L'_A M'_A L'_B M'_B S'_N\rangle$. The decay width is given as before by Eq. (7). Retaining the leading term as $R \to \infty$ we again obtain the decay amplitude as the product of amplitudes of processes occurring in the individual atoms: dipole allowed deexcitation of the dication A and ionization of B. The resulting expression for the partial width Γ_i takes on the form given in Eq. (14). In this case the line strength $S_i^{(A)}(E'_A L'_A; E_A L_A)$ should be interpreted as pertaining to the relevant transition in the dication with ω_i being corresponding excitation energy. The total width is again obtained by summing all partial widths.

C. Excited neutral atom A

Below we discuss the asymptotic decay widths for excited states in the neutral cluster AB (see Fig. 1). The initial state $|EL_A M_A S_A\rangle$ is usually produced through single-photon absorption. We assume that it is singly excited, and at large interatomic distances this excitation is localized on atom A. We consider an electron from the shell nv to be excited onto the shell ip. The shell nv can be either outer valence or inner valence, while ip refers to a bound virtual orbital of A. It can be constructed analogously to the cases described above, such that $L_A = 1$ and $S_A = 0$. There are several types of final states coupled to this initial state in the lowest order of perturbation theory which correspond to different decay pathways. One is for atom A to revert to its ground state simultaneously ionizing the atom B. The final state given by the wave function $|E'L'_B M'_B S'\rangle$ has a hole in ov_B shell of the atom B with an electron in the electronic continuum. For excitations from the outer valence shell we call this process excitation transfer ionization (ETI) [8], while for excitations from inner-valence orbitals it is named *participator* resonant interatomic Coulombic decay (pRICD) [9]. Another possibility may arise only if an inner-valence electron is excited in the initial state. Then, an electron from the outer-valence shell ov_A of A might fill the inner-valence vacancy, thereby ionizing the neighboring atom B. The final state $|E'L'_A M'_A L'_B M'_B S'_N\rangle$ will comprise a hole in the shell ov_A and an electron in the shell ip of the atom A, a hole in the shell ov_B of the atom B, and an electron in the continuum. This process is called *spectator* resonant ICD or sRICD [9].

The decay width is given again by Eqs. (14) and (16). The line strength $S_i^{(A)}(E'_A L'_A; E_A L_A)$ and transition energies ω_i correspond to the deexcitation of the initial state in the case of ETI or pRICD or to the transition between the outer- and inner-valence shells in the case of sRICD.

III. APPLICATION TO SPECIFIC SYSTEMS AND DISCUSSION

A. ICD in CaHe following $3p$ ionization of Ca

We apply now the asymptotic formulas obtained in the preceding sections to concrete systems and compare the results with *ab initio* calculations. An interesting aspect of this comparison is the range of validity of the asymptotic expansion. We start with the ICD in the system addressed in the Introduction: $\mathrm{Ca}^+(3p^{-1})\mathrm{He}$. The initial states are of $^2\Sigma^+$ and $^2\Pi$ symmetry which arise from a $^2P^o$ term of Ca^+ and ^1S term of He and, therefore, $L_A = 1$. The final state is given by $\mathrm{Ca}^+(4s^{-1})\mathrm{He}^+ + e$. There is only one accessible interatomic decay channel with $\mathrm{ov}_A = 4s$ and, hence, $L'_A = 0$. Thus, using Eq. (14) we obtain for the coefficients P_{M_A} of the states polarized along ($M_A = 0$) and perpendicular ($M_{iv} = \pm 1$) to the z axis the following values: $P_0 = 4/3$, $P_{\pm 1} = 1/3$. The ratio of the decay widths of these states is consequently

$$\frac{\Gamma_0}{\Gamma_{\pm 1}} = 4. \quad (18)$$

In this case one can illustrate the decay by a simple one-electron picture (see Fig. 2). The initial state polarized along the z axis has a hole in the $3p_z$ orbital of Ca. The only decay pathway operative at large interatomic distances is for an electron from the $4s$ orbital to fill this vacancy. The transition dipole should be oriented parallel to z axis and, according to Eq. (10), the induced dipole on He atom will be also parallel to it. If, on the other hand, the initial state is polarized perpendicular to the z axis, the hole is on the $3p_{\pm 1}$ orbital
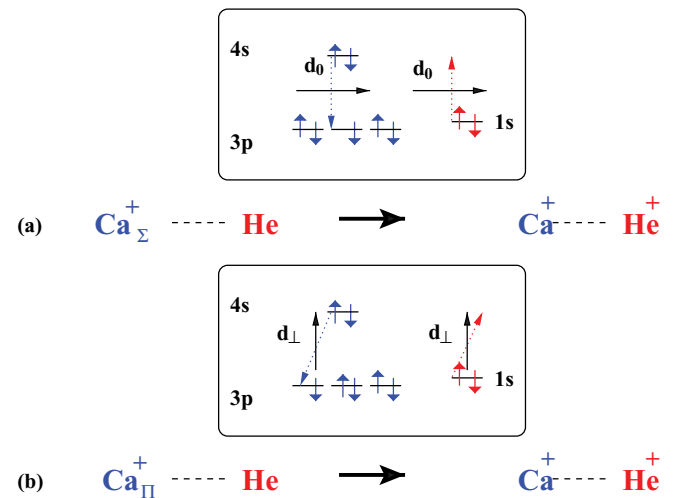

FIG. 2. (Color online) Schematic representation of the interatomic decay in $\mathrm{Ca}^+(3p^{-1})\mathrm{He}$. (a) Decay of $^2\Sigma$ state and (b) decay of $^2\Pi$ state. The symbols d_0 and $d_\perp$ stand for the components of the one-particle dipole operator parallel and perpendicular to the interatomic axis, respectively.
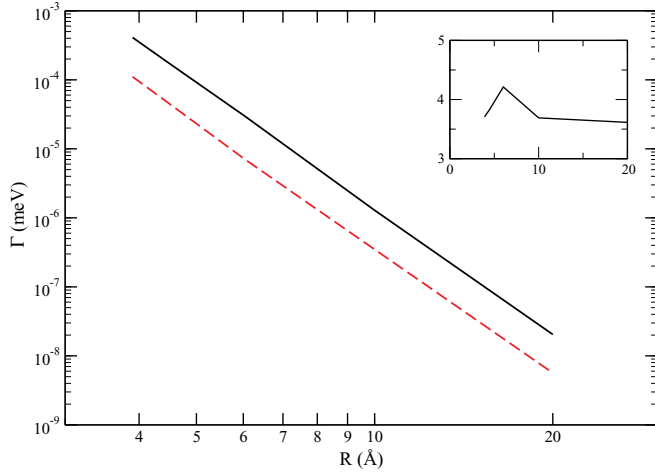
FIG. 3. (Color online) Double logarithmic graph of the *ab initio* ICD widths of Ca$^+$($3p^{-1}$)He as a function of interatomic distance *R*. The solid line is the decay width of the $^2\Sigma$ state; the broken line is the decay width of the $^2\Pi$ state. The inset shows the ratio $\Gamma_{2\Sigma}/\Gamma_{2\Pi}$ as a function of interatomic distance. The asymptotic formulas predict a ratio equal to 4. The minimum of the potential energy curve in the electronic ground state of CaHe is at 6 Å.

and both the transition dipole on Ca$^+$ and the induced dipole on He are also perpendicular to the *z* axis. Since, according to Eq. (11) the dipoles parallel to the *z* axis interact twice as strongly as those perpendicular to it the ratio of the decay widths will indeed be 4. This value is the greatest one can obtain for the ratio of the decay widths at large interatomic distances. It is possible only if the decay of the state of one polarization is driven exclusively by the *z* component of the dipole moment, while the decay of the state of the other polarization is correspondingly driven by the *x* component.

We compare this asymptotic result with calculations done by the Fano-ADC-Stieltjes method, where many-body Green's function technique is used to solve the many-body Schrödiger equation, Fano formalism is applied to obtain decay widths, and Stieltjes imaging is used to renormalize the discretized continuum (see Ref. [28] for details). The particulars of the computation can be found in Ref. [18]. The results are summarized in Fig. 3. We see that the numerical ratio of the decay widths stays about 3.75 at large *R*'s. Surprisingly, it remains close to 4 even about the equilibrium interatomic distance. The explanation seems to be that the equilibrium distance of Ca$^+$($3p^{-1}$)He at 4 Å is clearly larger than 2.1 Å which is the sum of atomic radii of Ca and He atoms. Thus, the orbital overlap, which is the primary cause for the deviation from the asymptotic behavior [4] still does not play any significant role at the equilibrium distance.

So far there have been no direct measurements of ICD widths for dimers. However, we argue that the difference in the decay width due to the different symmetry of the decaying state will give rise to observable effects in the experiments used currently to study ICD. One of the techniques employed is called COLTRIMS (cold target recoil ion momentum spectroscopy) method [29]. It relies on the fact that the final dicationic state of ICD is unstable and undergoes Coulomb explosion. Thus, following the emission of the primary photoelectron,

the secondary ICD electron is observed in coincidence with the arrival of two positively charged ions, e.g., Ca$^+$ and He$^+$ to use the example above. The measured quantities are the kinetic energy of the ICD electron (ICD spectrum) and the kinetic energy of the ions (kinetic energy release or KER), whose sum should remain constant due to energy conservation. The ICD electron can be observed over the full solid angle for a selected alignment of the interatomic axis. Knowing this alignment the polarization of the radiation used to prepare the decaying state can be chosen to produce the state of either Σ or Π symmetry. For how to compute the ICD spectrum taking into account the motion of the nuclei along the interatomic axis see Ref. [30] and references therein. It follows from it that increasing Γ *n*-fold will lead to the *n*-fold increase in the ICD spectrum's intensity, provided one can neglect the difference between Σ and Π electronic potential energy surfaces and that ICD does not perturb vibrational wave functions considerably. Therefore, in the example above the ICD spectrum of the Σ state should have the same structure but four times the intensity of the one of the Π state. Similar experiment will be possible in the case of the ICD after Auger decay, where Coulomb explosion likewise takes place. However, the COLTRIMS method is not directly applicable to the case of ICD in neutral excited clusters where no Coulomb explosion follows the electronic decay.

B. ICD after Auger in the NeMg cluster following Auger decay in Ne

We next consider the application of the asymptotic formulas to the ICD after Auger decay in the NeMg cluster. The initial state is characterized by the vacancies in $2s$ and $2p$ shells of the Ne atom. Both $^1P^o$ and $^3P^o$ terms were observed after Auger decay in isolated Ne [26], and they in turn give rise to $^{1,3}\Sigma^+$ and $^{1,3}\Pi$ states of Ne^{2+}Mg. In the interatomic Coulombic decay of Ne^{2+}($2s^{-1}2p^{-1}$)Mg one of the $2p$ electrons of Ne fills the $2s$ vacancy to give the following electronic configuration in the final state: Ne^{2+}($2p^{-2}$)Mg$^+$($3s^{-1}$) + e. There are two equivalent holes in the $2p$ shell of Ne corresponding to ^1S, ^3P, and ^1D atomic terms [25] which in turn give rise to two $^1\Sigma^+$, $^1\Pi$, $^1\Delta$, $^3\Sigma^-$, and $^3\Pi$ molecular terms [31]. We consider first the decay of the singlet excited state of Ne^{2+}. The orbital angular-momentum values in the final state are $L'_A = 0$ and $L'_A = 2$, thus, there are two open ICD channels. The transition energies corresponding to these multiplets are $\omega_{1S} = 29.0$ eV and $\omega_{1D} = 32.7$ eV. Since the photoionization cross section of Mg varies slowly in this energy interval [32], we can replace in Eq. (14) these transition energies by the average value $\langle\omega\rangle$. Thus, using Eqs. (14) and (17), we obtain for the decay widths

$$\Gamma_{1\Sigma} = \frac{c}{2\pi\langle\omega\rangle R^6}\sigma^{(Mg)}(\langle\omega\rangle)$$
$$\times \left(\frac{4}{3}S^{(Ne^{2+})}(1;0) + \frac{11}{15}S^{(Ne^{2+})}(1;2)\right) \quad (19a)$$

$$\Gamma_{1\Pi} = \frac{c}{2\pi\langle\omega\rangle R^6}\sigma^{(Mg)}(\langle\omega\rangle)$$
$$\times \left(\frac{1}{3}S^{(Ne^{2+})}(1;0) + \frac{19}{30}S^{(Ne^{2+})}(1;2)\right) \quad (19b)$$

of the initial states polarized parallel and perpendicular to the z axis, respectively. The line strengths $S^{(Ne^{2+})}(L_A; L'_A)$ correspond to the transitions between multiplets discussed above.

One can also show that in the case of one-determinant approximation used to construct the wave functions the ratio of the line strengths $S^{(Ne^{2+})}(0 \leftarrow 1)$ and $S^{(Ne^{2+})}(2 \leftarrow 1)$ corresponding to the transitions to different final states is exactly 1:5. Therefore, we find for the decay widths's ratio

$$\frac{\Gamma_{^1\Sigma}}{\Gamma_{^1\Pi}} = \frac{10}{7} \approx 1.43. \tag{20}$$

We analyze the decay of the ^3P initial state of Ne^{2+} in a similar way. The only available final state is the ^3P term of $Ne^{2+}(2p^{-2})$, thus $L'_A = 1$. The ratio $\Gamma_{^3\Sigma} / \Gamma_{^3\Pi}$ is found to be

$$\frac{\Gamma_{^3\Sigma}}{\Gamma_{^3\Pi}} = \frac{2}{5}. \tag{21}$$

We immediately notice that in the triplet case $^3\Pi$ state decays faster than $^3\Sigma^+$ state which is the opposite to what is happening in the case of the singlet.

Surprisingly, one can obtain the same ratios employing simple considerations and using only addition and division of integers. To this end one should consider the deexcitation of A in terms not of the atomic but of the corresponding molecular states. We designate by **d** the one particle dipole operator with the components d_0 and $d_{\pm1} \equiv d_\perp$. In the singlet spin case the dipole transitions from the initial $^1\Sigma^+$ state are allowed to two $^1\Sigma^+$ and one $^1\Pi$ final states. It is easy to check that the transitions to $^1\Sigma^+$ states are driven by d_0 and to $^1\Pi$ by $d_\perp$. In the case of $^1\Pi$ initial state the allowed transitions are to two $^1\Sigma^+$, one $^1\Pi$, and one $^1\Delta$ states, where only the transition to $^1\Pi$ is driven by d_0, the rest are by $d_\perp$. In the transition from Σ to Π state two final states with projections $\Pi = \pm1$ are accessible in dipole approximation. Similar considerations show that in the other cases there is only one final state accessible in the dipole approximation. Estimating the contribution to Γ of each transition driven by d_0 as four times that driven by $d_\perp$ we arrive at $\Gamma_{^1\Sigma} / \Gamma_{^1\Pi} = 10/7$ which is the result obtained above. In the case of triplet spin the initial $^3\Sigma^+$ state can only decay to $^3\Pi$ final state, the transition to $^3\Sigma^-$ being forbidden [31]. The decay of the $^3\Pi$ state can proceed both to the $^3\Sigma^-$ and $^3\Pi$ states. Summing up contributions of different transitions to the corresponding decay widths we obtain the ratio of 2 to 5 in agreement with the procedure above. This simple method of finding ratios of the decay widths will produce good results as long as the final states are all derived from the same electronic configuration and electron correlation can be neglected.

We again compare the asymptotic results with Fano-ADC-Stieltjes calculations of interatomic decay in $Ne^{2+}(2s^{-1}2p^{-1})Mg$ reported in Ref. [17]. In Fig. 4 we see the decay widths in the case of the spin singlet initial state. These decay widths exhibit $1/R^6$ behavior at interatomic distances larger than 9 Å, effects of orbital overlap becoming operative at smaller values of R. The inset shows the ratio of $\Gamma_{^1\Sigma}$ to $\Gamma_{^1\Pi}$. At $R > 9$ Å it oscillates about the theoretical value of 1.43 and increases for smaller R's. This growth can be explained by the effect of orbital overlap which should be more pronounced in the case of the state oriented along z axis, i.e., $^1\Sigma$ state. In the case of the triplet states's decay in Fig. 5
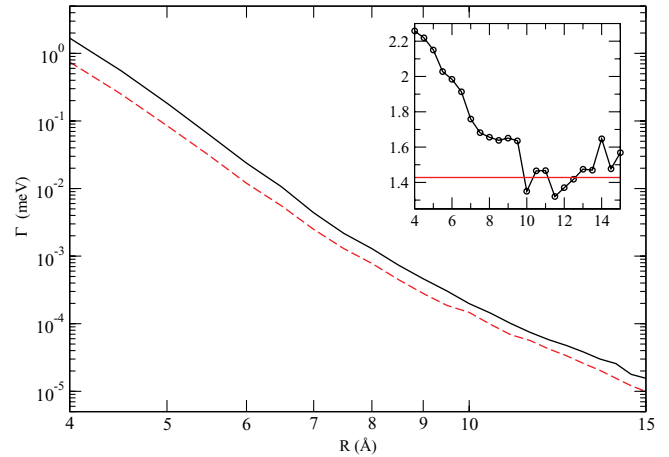

FIG. 4. (Color online) Double logarithmic graph of the *ab initio* ICD widths of the singlet excited states in ICD after Auger decay in $Ne^{2+}(2s^{-1}2p^{-1})Mg$ as a function of interatomic distance R. The solid line is the decay width of the $^1\Sigma$ state; the broken line is the decay width of the $^1\Pi$ state. The inset shows the ratio $\Gamma_{^1\Sigma} / \Gamma_{^1\Pi}$ as a function of interatomic distance. The horizontal line at 1.428 is the theoretical result predicted by the asymptotic formulas (see text). The minimum of the potential energy curve in the electronic ground state is at 4.4 Å.

we see again that at large interatomic distances the ratio of the decay widths agrees to an excellent degree with the asymptotic value of 0.4. As R decreases and the orbital overlap becomes significant this ratio grows due to orbital overlap, until at about 5 Å the corresponding widths become equal. Thus, the orbital overlap cancels the effect of the dipole-dipole interaction on the $\Gamma_{^3\Sigma} / \Gamma_{^3\Pi}$ ratio. Since both the Auger and ICD processes are usually faster than the nuclear motion the interatomic decay happens at about equilibrium interatomic distance of neutral NeMg of 4.4 Å. Therefore, in the experiment one should not expect to observe pronounced difference between $\Gamma_{^3\Sigma}$ and
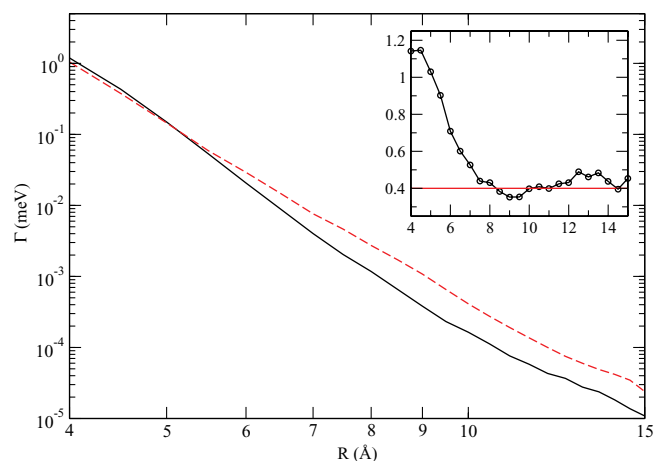

FIG. 5. (Color online) Double logarithmic graph of the *ab initio* ICD widths of the triplet excited state in ICD after Auger decay in $Ne^{2+}(2s^{-1}2p^{-1})Mg$ as a function of interatomic distance R. The solid line is the decay width of the $^3\Sigma$ state; the broken line is the decay width of the $^3\Pi$ state. The inset shows the ratio $\Gamma_{^3\Sigma} / \Gamma_{^3\Pi}$ as a function of interatomic distance. The horizontal line at 0.4 is the theoretical result predicted by the asymptotic formulas (see text).

$\Gamma_{^3\Pi}$ unlike in the case of spin singlet, where the effects of dipole-dipole interaction and the orbital overlap do not cancel each other.

In the case considered above the final state comprises two holes on Ne in the same $2p$ shell. These holes represent the so-called equivalent particles. In constructing atomic terms from two equivalent particles, for example, in the spin singlet case, the Pauli exclusion principle forbids the term ^1P. If the two holes were in two different shells np and $n'p$ ^1P term would be allowed, and the widths's ratio would be equal to unity. Mathematically the case of two nonequivalent holes in ICD after Auger decay is identical with that of sRICD considered below.

C. ICD in NeMg cluster following the excitation of a *2s* electron of Ne

As the last example we consider the decay of the inner-valence excited state in neutral NeMg cluster investigated in Ref. [9]. The initial state is obtained by promoting a $2s$ electron of Ne into a vacant $3p$ orbital. The resulting atomic $^1P^o$ ($L_A = 1$) term splits into $^1\Sigma^+$ and $^1\Pi$ molecular terms in NeMg cluster. In the decay of Ne($2s^{-1}3p$)Mg according to sRICD pathway a $2p$ electron of Ne fills the $2s$ vacancy, and a $3s$ electron of Mg is simultaneously ionized. The final state is given by Ne($2p^{-1}3p$)Mg($3s^{-1}$) $+ e$. We see that in the final state the Ne atom remains in the excited state with a hole in a $2p$ and and electron in a $3p$ orbital. There are three atomic terms which correspond to this configuration and are accessible from the initial state: ^1S, ^1P, ^1D ($L'_A = 0,1,2$), which in their turn give rise to the following molecular terms of the complete system: two $^1\Sigma^+$, two $^1\Pi$, $^1\Sigma^-$, $^1\Delta$. Their energies lie within an interval of 0.3 eV about 18.55 eV, where $\sigma^{(\text{Mg})}(\omega)$ remains almost constant, therefore, we may again use the average value $\langle\omega\rangle$ in Eq. (14) to obtain

$$
\begin{aligned}
\Gamma_{^1\Sigma} = \frac{c}{2\pi\langle\omega\rangle R^6}\sigma^{(\text{Mg})}(\langle\omega\rangle) \\
\times \left(\frac{4}{3}S^{(\text{Ne})}(1;0) + \frac{2}{6}S^{(\text{Ne})}(1;1) + \frac{11}{15}S^{(\text{Ne})}(1;2)\right)
\end{aligned}
\tag{22a}
$$

$$
\begin{aligned}
\Gamma_{^1\Pi} = \frac{c}{2\pi\langle\omega\rangle R^6}\sigma^{(\text{Mg})}(\langle\omega\rangle) \\
\times \left(\frac{1}{3}S^{(\text{Ne})}(1;0) + \frac{5}{6}S^{(\text{Ne})}(1;1) + \frac{19}{30}S^{(\text{Ne})}(1;2)\right).
\end{aligned}
\tag{22b}
$$

Again we can show that in the one determinant approximation the ratio of the line strengths pertaining to the transitions to different multiplets $S^{(\text{Ne})}(1;0) : S^{(\text{Ne})}(1;1) : S^{(\text{Ne})}(1;2)$ is 1:3:5 giving the widths ratio

$$
\frac{\Gamma_{^1\Sigma}}{\Gamma_{^1\Pi}} = 1.
\tag{23}
$$

If Ne($2s^{-1}3p$)Mg decays by pRICD pathway the $3p$ electron fills the initial $2s$ vacancy simultaneously ionizing a $3s$ electron of Mg. The final state of Ne is its ground state which is assumed to be of ^1S symmetry giving rise to the $^1\Sigma^+$
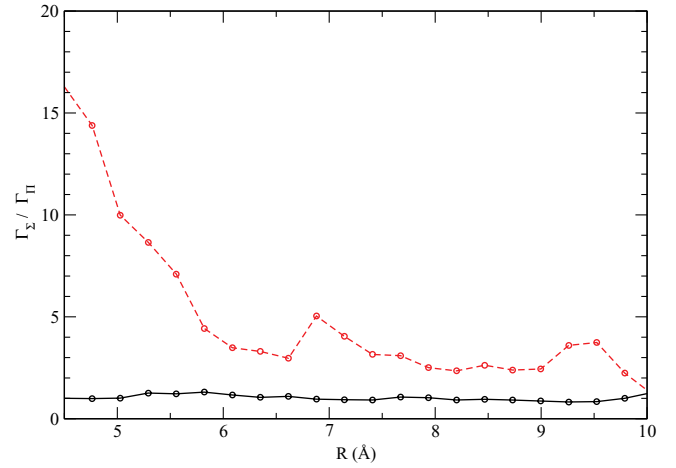

FIG. 6. (Color online) Ratio of the *ab initio* ICD widths of $^1\Sigma$ and $^1\Pi$ states in sRICD and pRICD in Ne($2s^{-1}3p$)Mg. The solid line is the ratio of sRICD widths; the broken line is the ratio of pRICD widths. The respective asymptotic values are 1 and 4, respectively.

and $^1\Pi$ molecular terms. Applying Eq. (14) we obtain

$$
\frac{\Gamma_{^1\Sigma}}{\Gamma_{^1\Pi}} = 4.
\tag{24}
$$

We compare the asymptotic results with the *ab initio* calculations which were reported in Ref. [9]. In them, unlike in the Fano-ADC calculations for the cases of the singly and doubly ionized clusters considered above, we used single determinant initial and final states. Therefore, the results obtained are expected to be less precise than those obtained by the Fano-ADC method. The respective ratios of the decay widths are plotted in Fig. 6. We see that the ratio of sRICD width oscillates slightly about the predicted asymptotic value of 1 down to the interatomic distances comparable with the equilibrium distance of about 3.5 Å. In this respect sRICD is similar to the ICD in the corresponding singly ionized cluster. Indeed, since the $3p$ electron does not participate in the decay, sRICD is just an ICD in the presence of an "observer." The orbital overlap which could alter the ratio of the decay widths is in the case of ICD the overlap between occupied orbitals localized close to the respective nuclei and does not become pronounced until distances comparable with the sum of the atomic radii of constituent species. In the case of pRICD the *ab initio* calculations produce the ratio of Γ's which oscillates about the value 3 instead of predicted 4. A possible explanation could be the poorer quality of numerical results in the pRICD case, where the $3p$ electron participates in the decay, compared with the sRICD case. This is ultimately related to the inadequate description of virtual orbitals in a single determinant approximation. At smaller interatomic distances we see the already familiar enhancement of the decay of $^1\Sigma^+$ state compared with the decay of $^1\Pi$ one. However, this enhancement is much more pronounced than the one we observed in the ICD after Auger decay. This is in turn related to the more pronounced orbital overlap effects, where a delocalized virtual orbital participating in the decay is involved, compared to the localized hole orbitals in the ICD after Auger decay.

IV. CONCLUSIONS

In this article, we investigated the dependence of the widths of interatomic Coulombic decay in a heteronuclear diatomic AB on the symmetry of the decaying state. We concentrated here on decaying states which in the free atom A can decay radiatively by emitting a single photon. We were particularly interested in the states of P symmetry which is split in AB into two molecular terms of symmetries Σ and Π. We derived analytical expressions for the decay widths of these molecular states in the limit of large interatomic distances. In this limit the amplitude of the ICD process is given as the product of the dipole amplitudes of the processes occurring on the isolated atoms A and B; these are the deexcitation of A and the ionization of B connected through the transfer of the "virtual" photon. The partial decay width for an open ICD channel, thus, falls off as $1/R^6$ with the interatomic distance and is proportional to the product of the line strength of the corresponding transition on A and the photoinization cross section of B at the virtual photon's energy. Moreover, this width is multiplied by a prefactor depending on the symmetry of the decaying state. As we showed this dependence is related to the dependence of the interaction energy of two classical dipoles on their mutual orientation. The asymptotic widths do not depend on the way the system undergoing ICD was produced. The same expressions were obtained for excited singly ionized, doubly ionized, and neutral clusters.

We applied the asymptotic expressions to ICD in selected excited singly ionized, doubly ionized, and neutral clusters. Calculated ratios of $\Gamma_\Sigma / \Gamma_\Pi$ depend on the number of available ICD channels, and the symmetry and spin of the final states. Thus, in ICD of singly ionized CaHe cluster, the only available final state is of $^2\Sigma^+$ symmetry. The obtained ratio is equal to 4, the highest value possible in the framework of the virtual photon model. In the case of ICD after Auger decay in the NeMg cluster, the singlet decaying state is coupled to several final states and the resulting ratio is about 1.43, while for the triplet state it becomes 0.4. The surprising aspect of these widths's ratios is that they are independent of the interatomic distance, while the ratios of electronic energies E_Σ/E_Π goes to 1 as R increases. This is related to the fact that, as noted above, the ratio of the interaction energies of two classical dipoles depends on the mutual orientation of the latter but is independent of the distance between them.

The asymptotic results were compared to *ab initio* calculations for the systems of investigated. We found a good agreement between the asymptotic and numerical results for large interatomic distances where orbital overlap can be neglected. At smaller R effects of orbital overlap can be observed which lead to enhancement of Γ_Σ over Γ_Π. It may lead to the significant increase of the corresponding ratio at equilibrium interatomic distances, as for example in the pRICD case in NeMg. It can also cancel any difference between the decay widths as in the case of decay of the triplet states in ICD after Auger decay in NeMg. We also discussed the ways the difference in the decay width due to the different symmetry of the initial state can be measured using the COLTRIMS technique common in studying the ICD process. This technique seems to be directly applicable to measurements in singly and doubly ionized clusters but not to neutral excited ones.

In this work we considered an important class of systems. It would be interesting to investigate the dependence of the decay width on the symmetry also in homonuclear dimers such as Ne_2. Another important class of systems worth considering are those with dipole forbidden decaying states, where the leading term in the asymptotic expansion corresponds to a quadrupole transition.

APPENDIX: DERIVATION OF THE ASYMPTOTIC FORMULAE

1. Singly ionized clusters

In this Appendix we present the derivation of the asymptotic formulas for the interatomic decay widths. We do it in detail only for the case of ICD in a singly ionized cluster, while for the rest of the processes we only indicate where the derivation deviates from it. Definitions and assumptions made in Sec. II remain valid here. The initial spin doublet 1h state of ICD is

$$|E L_A M_A S M_S\rangle = \hat{c}_{\alpha_{iv}} |\Phi_0\rangle. \tag{A1}$$

The final 1p2h states are constructed in two steps. First, one constructs spin eigenfunctions of the total spin operator

$$\left|\beta_\epsilon \alpha_{\text{ov}_A} \beta_{\text{ov}_B}; S'_N M'_S\right\rangle = \sum_{\mu_\epsilon \mu_{\text{ov}_A} \mu_{\text{ov}_B}} C^{S'_N M'_S}_{\mu_\epsilon \mu_{\text{ov}_A} \mu_{\text{ov}_B}} \hat{c}^\dagger_{\beta_\epsilon} \hat{c}_{\alpha_{\text{ov}_A}} \hat{c}_{\beta_{\text{ov}_B}} |\Phi_0\rangle, \tag{A2}$$

where $S'_N = 1/2$. Spin coupling coefficients $C^{S'_N M'_S}_{\mu_\epsilon \mu_{\text{ov}_A} \mu_{\text{ov}_B}}$ correspond to the following coupling schemes: for $N = 1$ adding holes's spins to form a singlet, then adding electron spin to form a doublet, for $N = 2$ adding holes's spins to form a triplet, then adding electron spin to form a doublet. Second, one sums orbital angular momenta of the particles localized on A or B, respectively, to obtain

$$|E' L'_A M'_A L'_B M'_B S'_N M'_S\rangle = \sum_{m_\epsilon m_{\text{ov}_B}} C^{L'_B M'_B}_{m_\epsilon m_{\text{ov}_B}} \left|\beta_\epsilon \alpha_{\text{ov}_A} \beta_{\text{ov}_B}; S'_N M'_S\right\rangle, \tag{A3}$$

where $C^{L'_B M'_B}_{m_\epsilon m_{\text{ov}_B}}$ are expressed through the standard Clebsch-Gordan coefficients of the rotation group as

$$C^{L'_B M'_B}_{m_\epsilon m_{\text{ov}_B}} = (-1)^{m_{\text{ov}_B}} \left(l_\epsilon m_\epsilon l_{\text{ov}_B} - m_{\text{ov}_B} | l_\epsilon l_{\text{ov}_B} L'_B M'_B\right). \tag{A4}$$

The decay width is given by

$$\Gamma = 2\pi \sum \left|\langle E' L'_A M'_A L'_B M'_B S'_N | \hat{V}_e | E L_A M_A S\rangle\right|^2 \delta(E' - E), \tag{A5}$$

where the sum runs over all final states available for ICD and averaging over different spin projections in the initial state is implied. The operator $\hat{V}_e$ is an electron-electron interaction given by

$$\hat{V}_e = \frac{1}{2} \sum_{i \neq j} \frac{1}{|\mathbf{r_i} - \mathbf{r_j}|}, \qquad (A6)$$

where $\mathbf{r}_i$ are the coordinates of the i-th electron. Introducing Eq. (A4) into Eq. (A5) we obtain Γ as a linear combination of spin-reduced matrix elements $\langle \beta_\epsilon \alpha_{\mathrm{ov}_A} \beta_{\mathrm{ov}_B}; S_N' | \hat{V}_e | E L_A M_A S \rangle$ which can be evaluated using Eqs. (A1) and (A2) and the Condon-Slater rules [33]. For our choice of spin coupling schemes we obtain

$$\langle \beta_\epsilon \alpha_{\mathrm{ov}_A} \alpha_{\mathrm{ov}_B} S_I' | \hat{V}_e | E L_A M_A S \rangle$$
$$= \frac{1}{\sqrt{2}} \left(V_{\alpha_{\mathrm{iv}} \beta_\epsilon \alpha_{\mathrm{ov}_A} \beta_{\mathrm{ov}_B}} + V_{\alpha_{\mathrm{iv}} \beta_\epsilon \alpha_{\mathrm{ov}_B} \beta_{\mathrm{ov}_A}} \right) \qquad (A7a)$$

$$\langle \beta_\epsilon \alpha_{\mathrm{ov}_A} \alpha_{\mathrm{ov}_B} S_{II}' | \hat{V}_e | E L_A M_A S \rangle$$
$$= \sqrt{\frac{3}{2}} \left(V_{\alpha_{\mathrm{iv}} \beta_\epsilon \alpha_{\mathrm{ov}_A} \beta_{\mathrm{ov}_B}} - V_{\alpha_{\mathrm{iv}} \beta_\epsilon \alpha_{\mathrm{ov}_B} \beta_{\mathrm{ov}_A}} \right), \qquad (A7b)$$

where

$$V_{ijkl} = \int d\mathbf{r_1} d\mathbf{r_2} \phi_i^*(\mathbf{r_1}) \phi_j^*(\mathbf{r_2}) \frac{1}{|\mathbf{r_1} - \mathbf{r_2}|} \phi_k(\mathbf{r_1}) \phi_l(\mathbf{r_2}) \qquad (A8)$$

and ϕ_n is a spatial part of the spin-orbital $|\gamma_n l_n m_n \mu_n\rangle$. Matrix element $V_{\alpha_{\mathrm{iv}} \beta_\epsilon \alpha_{\mathrm{ov}_B} \beta_{\mathrm{ov}_A}}$ falls off exponentially with interatomic distance, since orbitals $|\alpha_{\mathrm{iv}} l_{iv} m_{\mathrm{iv}} \mu_{\mathrm{iv}}\rangle$ and $|\beta_{\mathrm{ov}_B} l_{\mathrm{ov}_B} m_{\mathrm{ov}_B} \mu_{\mathrm{ov}_B}\rangle$ are localized on different atoms. We neglect it in the asymptotic expansion to obtain

$$\langle \beta_\epsilon \alpha_{\mathrm{ov}_A} \alpha_{\mathrm{ov}_B}; S_N | \hat{V}_e | \alpha_{\mathrm{iv}} L_{iv} M_{\mathrm{iv}}; S \rangle = C_N V_{\alpha_{\mathrm{iv}} \beta_\epsilon \alpha_{\mathrm{ov}_A} \beta_{\mathrm{ov}_B}}, \qquad (A9)$$

where $C_I = 1/\sqrt{2}$ and $C_{II} = \sqrt{3/2}$. For the matrix element in Eq. (A9) not to be exponentially small at large interatomic distances one electron should be localized on A and the other on B. We denote corresponding electron coordinates as $\mathbf{r_A}$ and $\mathbf{r_B}$ instead of $\mathbf{r_1}$ and $\mathbf{r_2}$ to emphasize this (see Fig. 7). Choosing the coordinate origin at the position of atom A we see that asymptotically $|\mathbf{r_A}| < |\mathbf{r_B}|$, and we might use the following expansion of $1/|\mathbf{r_A} - \mathbf{r_B}|$ in terms of spherical harmonics [23]

$$\frac{1}{|\mathbf{r_A} - \mathbf{r_B}|} = 4\pi \sum_{l=0}^{\infty} \sum_{m=-l}^{l} \frac{1}{2l+1} \frac{r_A^l}{r_B^{l+1}} Y_{lm}^*(\Omega_B) Y_{lm}(\Omega_A). \qquad (A10)$$

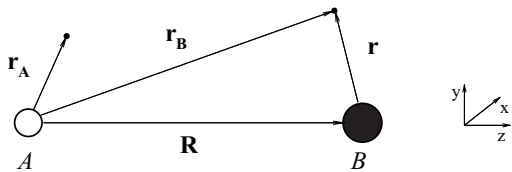
FIG. 7. Two atoms A and B lie on the z axis at a distance R from each other. The vector $\mathbf{r}_A$ denotes the coordinate of an electron localized on the atom A, while $\mathbf{r}_B$ and $\mathbf{r}$ stand for the coordinate of an electron localized on the atom B.

Inserting it into Eq. (A9) we obtain

$$\langle \beta_\epsilon \alpha_{\mathrm{ov}_A} \alpha_{\mathrm{ov}_B}; S_N' | \hat{V}_e | E L_A M_A S \rangle$$
$$= 4\pi C_N \sum_{l=0}^{\infty} \sum_{m=-l}^{l} \frac{1}{2l+1} \langle \phi_{\mathrm{iv}} | Y_{lm}(\Omega_A) r_A^l | \phi_{\mathrm{ov}_A} \rangle$$
$$\langle \phi_\epsilon | \frac{Y_{lm}^*(\Omega_B)}{r_B^{l+1}} | \phi_{\mathrm{ov}_B} \rangle. \qquad (A11)$$

We see that at large interatomic distances matrix elements of the two-particle operator $\hat{V}_e$ can be represented as a product of matrix elements of two one-particle operators

$$\hat{D}_{lm}^{(A)} = \sqrt{\frac{4\pi}{2l+1}} \sum_{i \in A} Y_{lm}(\Omega_i) r_i^l \qquad (A12a)$$

$$\hat{D}_{lm}^{(B)} = \sqrt{\frac{4\pi}{2l+1}} \sum_{j \in B} Y_{lm}(\Omega_j)/r_j^{l+1} \qquad (A12b)$$

acting on the electron coordinates of either atom A or atom B. Introducing Eq. (A11) into Eq. (A9) and using Eq. (A2) we can express the amplitude of a given interatomic decay at large interatomic separation as the sum of products of amplitudes describing processes occurring on different atoms. Indeed, one obtains

$$\langle E' L_A' M_A' L_B' M_B' S_N' | \hat{V}_e | E L_A M_A S \rangle$$
$$= \frac{C_N}{\sqrt{2}} \sum_{l=0}^{\infty} \sum_{m=-l}^{l} \langle E_A' L_A' M_A' S_A' | \hat{D}_{lm}^{(A)} | E_A L_A M_A S_A \rangle$$
$$\times \langle \Phi_0^{(B)} | \hat{D}_{lm}^{(B)} | E_B' L_B' M_B' S_B' \rangle^*, \qquad (A13)$$

where $|E_A' L_A' M_A' S_A'\rangle$, $|E_A L_A M_A S_A\rangle$, and $|E_B' L_B' M_B' S_B'\rangle$ are the states of isolated atoms A and B constructed similarly to Eq. (A2), and $S_A' = 1/2$ and $S_B' = 0$. In Eq. (A13) the term with $l = 0$ is zero due to the orthogonality of the atomic wave functions. For $l = 1$, employing $Y_{10} = \sqrt{3/4\pi} \cos\theta$ and $Y_{1\pm1} = \mp\sqrt{3/8\pi} \sin\theta \exp\pm i\phi$ [20], we see that $\hat{D}_{1m}^{(A)}$ becomes just a transition dipole operator

$$\hat{D}_{1m}^{(A)} = \sum_{i \in A} r_m^{(i)}, \qquad (A14)$$

where

$$r_0 = z, \quad r_{\pm1} = \mp \frac{1}{\sqrt{2}}(x \pm iy). \qquad (A15)$$

If the dipole transition between the states of A $|E_A' L_A' M_A' S_A'\rangle$ and $|E_A L_A M_A S_A\rangle$ is allowed, the term with $l = 1$ is the leading one and will be the only term retained in the following calculations. Expanding $1/r_B$ in $\hat{D}_{1m}^{(B)}$ we obtain

$$\hat{D}_{1\pm1}^{(B)} = \frac{r_{\pm1}}{R^3} + O\left(\frac{1}{R^4}\right) \qquad (A16a)$$

$$\hat{D}_{10}^{(B)} = \frac{1}{R^2} - \frac{2r_0}{R^3} + O\left(\frac{1}{R^4}\right). \qquad (A16b)$$

Introducing these equations into Eq. (A13) we see that the term $1/R^2$ has zero contribution due to the orthogonality of $|\Phi_0^{(B)}\rangle$ and $|E_B' L_B' M_B' S_B'\rangle$. Therefore, $\hat{D}_{1m}^{(B)}$ becomes in its turn

proportional to a dipole transition operator $\hat{D}_m^B = \sum_{i \in B} r_m^{(i)}$ giving for the leading term the expression in Eq. (10). Derivations in the case of other decay processes differ only in the definitions of the initial and final states, as well as the spin-reduced matrix elements. We list below both the states involved and the necessary matrix elements for the ICD after Auger decay, sRICD, and pRICD processes.

2. Doubly ionized clusters

In ICD after Auger decay the initial 2 h state is given by

$$|\alpha_{iv}\alpha_{ov_A}; SM_S\rangle = \sum_{\mu_{iv}\mu_{ov_A}} C_{\mu_{iv}\mu_{ov_A}}^{SM_S} \hat{c}_{\alpha_{iv}} \hat{c}_{\alpha_{ov_A}} |\Phi_0\rangle \quad (A17a)$$

$$|EL_AM_ASM_S\rangle = \sum_{m_{iv}m_{ov_B}} C_{m_{iv}m_{ov_A}}^{L_AM_A} |\alpha_{iv}\alpha_{ov_A}; SM_S\rangle. \quad (A17b)$$

The spin coupling coefficients are obtained by coupling two spins 1/2 to form singlet or triplet spin state, while the coupling coefficients $C_{m_{iv}m_{ov_A}}^{L_AM_A}$ are given via Clebsch-Gordan coefficients of the rotation group as

$$C_{m_{iv}m_{ov_A}}^{L_AM_A} = (-1)^{m_{ov_A}+m_{iv}} \left(l_{iv} - m_{iv}l_{ov_A} - m_{ov_A}|l_{iv}l_{ov_A}L_AM_A\right). \quad (A18)$$

The final 1p3h states are given by

$$\begin{aligned}&|\alpha_{ov_A}\alpha_{ov'_A}\beta_\epsilon\beta_{ov_B}; S'_NM'_S\rangle \\ &= \sum_{\substack{\mu_{ov_A}\mu_{ov'_A}\\ \mu_\epsilon\mu_{ov_B}}} C_{\mu_{ov_A}\mu_{ov'_A}\mu_\epsilon\mu_{ov_B}}^{S'_NM'_S} \hat{c}_{\beta_\epsilon}^\dagger \hat{c}_{\beta_{ov_B}} \hat{c}_{\alpha_{ov_A}} \hat{c}_{\alpha_{ov'_A}} |\Phi_0\rangle\end{aligned}$$
$$(A19a)$$

$$\begin{aligned}&|E'L'_AM'_AL'_BM'_BS'_NM'_S\rangle \\ &= \sum_{\substack{m_{ov_A}m_{ov'_A}\\ m_\epsilon m_{ov_B}}} C_{m_{ov_A}m_{ov'_A}}^{L'_AM'_A} C_{m_\epsilon m_{ov_B}}^{L'_BM'_B} |\alpha_{ov_A}\alpha_{ov'_A}\beta_\epsilon\beta_{ov_B}; S'_NM'_S\rangle,\end{aligned}$$
$$(A19b)$$

where $C_{m_{ov_A}m_{ov'_A}}^{L'_AM'_A}$ is given by Eq. (A18), while $C_{m_\epsilon m_{ov_B}}^{L'_BM'_B}$ is given by Eq. (A4). The spin coupling coefficients correspond to the construction schemes in which first the spins of the three holes and then the spin of the particle are added together to obtain the total spin either of value 0 or 1. It is easy to check there are two possible construction schemes for $S = 0$ and three for $S = 1$. Corresponding spin-reduced matrix elements for $S = 0$ are

$$\langle \alpha_{ov_A}\alpha_{ov'_A}\beta_\epsilon\beta_{ov_B}; S'_I|\hat{V}_e|\alpha_{iv}\alpha_{ov_A}; S\rangle$$

$$= -\frac{1}{\sqrt{2}} \left(2V_{\beta_\epsilon\alpha_{iv}\beta_{ov_B}\alpha_{ov'_A}} - V_{\beta_\epsilon\alpha_{iv}\alpha_{ov'_A}\beta_{ov_B}}\right)$$

$$\langle \alpha_{ov_A}\alpha_{ov'_A}\beta_\epsilon\beta_{ov_B}; S'_{II}|\hat{V}_e|\alpha_{iv}\alpha_{ov_A}; S\rangle$$

$$= -\sqrt{\frac{3}{2}} V_{\beta_\epsilon\alpha_{iv}\alpha_{ov'_A}\beta_{ov_B}}, \quad (A20)$$

where all terms apart from the first one in the first equation decay exponentially with R. For the spin-reduced matrix

elements of the spin triplet states we obtain

$$\langle \alpha_{ov_A}\alpha_{ov'_A}\beta_\epsilon\beta_{ov_B}; S'_I|\hat{V}_e|\alpha_{iv}\alpha_{ov_A}; S\rangle$$

$$= -\frac{1}{\sqrt{6}} \left(2V_{\beta_\epsilon\alpha_{iv}\beta_{ov_B}\alpha_{ov'_A}} + V_{\beta_\epsilon\alpha_{iv}\alpha_{ov'_A}\beta_{ov_B}}\right)$$

$$\langle \alpha_{ov_A}\alpha_{ov'_A}\beta_\epsilon\beta_{ov_B}; S'_{II}|\hat{V}_e|\alpha_{iv}\alpha_{ov_A}; S\rangle$$

$$= \frac{1}{\sqrt{2}} V_{\beta_\epsilon\alpha_{iv}\alpha_{ov'_A}\beta_{ov_B}}$$

$$\langle \alpha_{ov_A}\alpha_{ov'_A}\beta_\epsilon\beta_{ov_B}; S'_{III}|\hat{V}_e|\alpha_{iv}\alpha_{ov_A}; S\rangle$$

$$= \frac{2}{\sqrt{3}} \left(V_{\beta_\epsilon\alpha_{iv}\beta_{ov_B}\alpha_{ov'_A}} - V_{\beta_\epsilon\alpha_{iv}\alpha_{ov'_A}\beta_{ov_B}}\right), \quad (A21)$$

where again the matrix elements $V_{\beta_\epsilon\alpha_{iv}\alpha_{ov'_A}\beta_{ov_B}}$ are exponentially small at large R and should be discarded.

3. Excited neutral clusters

For sRICD and pRICD processes the initial 1p1h state is given by

$$|\alpha_{ip}\alpha_{nv}; SM_S\rangle = \sum_{\mu_{ip}\mu_{nv}} C_{\mu_{ip}\mu_{nv}}^{SM_S} \hat{c}_{\alpha_{ip}}^\dagger \hat{c}_{\alpha_{nv}} |\Phi_0\rangle \quad (A22a)$$

$$|EL_AM_ASM_S\rangle = \sum_{m_{ip}m_{nv}} C_{m_{ip}m_{nv}}^{L_AM_A} |\alpha_{ip}\alpha_{nv}; SM_S\rangle, \quad (A22b)$$

where $S = 0$ and $C_{m_{ip}m_{nv}}^{L_AM_A}$ is given by Eq. (A4). The final 1p1h states of pRICD are given analogously by

$$|\beta_\epsilon\beta_{ov_B}; S'M'_S\rangle = \sum_{\mu_\epsilon\mu_{ov_B}} C_{\mu_\epsilon\mu_{ov_B}}^{S'M'_S} \hat{c}_{\beta_\epsilon}^\dagger \hat{c}_{\beta_{ov_B}} |\Phi_0\rangle \quad (A23a)$$

$$|E'L'_BM'_BS'M'_S\rangle = \sum_{m_\epsilon m_{ov_B}} C_{m_\epsilon m_{ov_B}}^{L'_BM'_B} |\beta_\epsilon\beta_{ov_B}; S'M'_S\rangle. \quad (A23b)$$

Spin-reduced matrix elements in the case of pRICD/ETI process are

$$\langle \beta_\epsilon\beta_{ov_B}; S'|\hat{V}_e|\alpha_{ip}\alpha_{nv}; S\rangle = 2V_{\beta_\epsilon\alpha_{nv}\beta_{ov_B}\alpha_{ip}} - V_{\beta_\epsilon\alpha_{nv}\alpha_{ip}\beta_{ov_B}},$$
$$(A24)$$

where again the last term decays exponentially at large R's. The final 2p2h states of sRICD are given by

$$\begin{aligned}&|\alpha_{ip}\alpha_{ov_A}\beta_\epsilon\beta_{ov_B}; S'_NM'_S\rangle \\ &= \sum_{\substack{\mu_{ip}\mu_{ov_A}\\ \mu_\epsilon\mu_{ov_B}}} C_{\mu_{ip}\mu_{ov_A}\mu_\epsilon\mu_{ov_B}}^{S'_NM'_S} \hat{c}_{\beta_\epsilon}^\dagger \hat{c}_{\alpha_{ip}}^\dagger \hat{c}_{\beta_{ov_B}} \hat{c}_{\alpha_{ov_A}} |\Phi_0\rangle \quad (A25a)\end{aligned}$$

$$\begin{aligned}&|E'L'_AM'_AL'_BM'_BS'_NM'_S\rangle \\ &= \sum_{\substack{m_{ip}m_{ov_A}\\ m_\epsilon m_{ov_B}}} C_{m_{ip}m_{ov_A}}^{L'_AM'_A} C_{m_\epsilon m_{ov_B}}^{L'_BM'_B} |\alpha_{ip}\alpha_{ov_A}\beta_\epsilon\beta_{ov_B}; S'_NM'_S\rangle.\end{aligned}$$
$$(A25b)$$

The coupling coefficients in Eq. (A25b) are given by Eq. (A4). The spin coupling coefficients are obtained first by coupling spins of two particles and two holes separately and by adding resulting spins to obtain singlet spin state of the four spin-1/2 particles. $N = 1$ corresponds to coupling the spins of the particles and holes producing singlets; $N = 2$ corresponds to coupling the spins of the particles and holes producing triplets. Corresponding spin reduced matrix elements are the same as in the ICD case and given in Eqs. (A7a) and (A7b).

[1] L. S. Cederbaum, J. Zobeley, and F. Tarantelli, Phys. Rev. Lett. **79**, 4778 (1997).

[2] R. Santra, J. Zobeley, and L. S. Cederbaum, Phys. Rev. B **64**, 245104 (2001).

[3] R. Santra and L. S. Cederbaum, Phys. Rep. **368**, 1 (2002).

[4] V. Averbukh, I. B. Müller, and L. S. Cederbaum, Phys. Rev. Lett. **93**, 263002 (2004).

[5] S. Marburger, O. Kugeler, U. Hergenhahn, and T. Möller, Phys. Rev. Lett. **90**, 203401 (2003).

[6] G. Öhrwall *et al.*, Phys. Rev. Lett. **93**, 173401 (2004).

[7] T. Jahnke *et al.*, Phys. Rev. Lett. **93**, 163401 (2004).

[8] K. Gokhberg, A. Trofimov, T. Sommerfeld, and L. S. Cederbaum, Europhys. Lett. **72**, 228 (2005).

[9] K. Gokhberg, V. Averbukh, and L. S. Cederbaum, J. Chem. Phys. **124**, 144315 (2006).

[10] S. Barth *et al.*, J. Chem. Phys. **122**, 241102 (2005).

[11] T. Aoto, K. Ito, Y. Hikosaka, E. Shigemasa, F. Penent, and P. Lablanquie, Phys. Rev. Lett. **97**, 243401 (2006).

[12] R. Santra and L. S. Cederbaum, Phys. Rev. Lett. **90**, 153401 (2003).

[13] Y. Morishita *et al.*, Phys. Rev. Lett. **96**, 243402 (2006).

[14] K. Kreidi *et al.*, J. Phys. B: At. Mol. Opt. Phys. **41**, 101002 (2008).

[15] K. Kreidi *et al.*, Phys. Rev. A **78**, 043422 (2008).

[16] S. D. Stoychev, A. I. Kuleff, F. Tarantelli, and L. S. Cederbaum, J. Chem. Phys. **129**, 074307 (2008).

[17] P. Kolorenc, V. Averbukh, K. Gokhberg, and L. S. Cederbaum, J. Chem. Phys. **129**, 244102 (2008).

[18] N. V. Kryzhevoi, V. Averbukh, and L. S. Cederbaum, Phys. Rev. B **76**, 094513 (2007).

[19] J. A. D. Matthew and Y. Komninos, Surf. Sci. **53**, 716 (1975).

[20] A. R. Edmonds, *Angular Momentum in Quantum Mechanics* (Princeton University Press, Princeton, NJ, 1974).

[21] R. Pauncz, *Spin Eigenfunctions* (Plenum Press, New York, 1979).

[22] U. Fano, Phys. Rev. **124**, 1866 (1961).

[23] J. D. Jackson, *Classical Electrodynamics*, 3rd ed. (Wiley, New York, 1998).

[24] M. Y. Amusia, *Atomic Photoeffect* (Springer, New York, 1990).

[25] I. I. Sobel'man, *An Introduction to the Theory of Atomic Spectra* (Pergamon Press, Oxford, 1972).

[26] A. Inoyatov *et al.*, J. Electron Spectrosc. Relat. Phenom. **154**, 79 (2007).

[27] M. Thompson, M. D. Baker, A. Christie, and J. Tyson, *Auger Electron Spectroscopy* (Wiley Interscience, New York, 1985).

[28] V. Averbukh and L. S. Cederbaum, J. Chem. Phys. **123**, 204107 (2005).

[29] A. Czasch *et al.*, Phys. Lett. **A347**, 95 (2005).

[30] S. Scheit *et al.*, J. Chem. Phys. **121**, 8393 (2004).

[31] G. Herzberg, *Molecular Spectra and Molecular Structure. I. Spectra of Diatomic Molecules* (Van Nostrand, New York, 1950).

[32] M. Y. Amusia *et al.*, J. Phys. B **10**, 1413 (1977).

[33] A. Szabo and N. Ostlund, *Modern Quantum Chemistry* (Dover, Mineola, NY, 1996).